Supporting Information

Prussian blue analogue-derived Ni and Co bimetallic oxide nanoplate arrays block-built from porous and hollow nanocubes for the efficient oxygen evolution reaction

Yan Shen,[c] Shu-Guang Guo,[b] Feng Du,[a] Xiao-Bo Yuan,[b] Yintong Zhang,[a] Jianqiang Hu,[c] Qing Shen,[d] Wenjun Luo,[c,e] Ahmed Alsaedi,[f] Tasawar Hayat,[f,g] Guihua Wen,[h] Guo-Ling Li,*[b] Yong Zhou,*[a,e,h] and Zhigang Zou[c,a,e,h]

[a] *National Laboratory of Solid State Microstructures, Collaborative Innovation Center of Advanced Microstructures, School of Physics, Nanjing University, Nanjing 210093, P. R. China. E-mail: zhouyong1999@nju.edu.cn*

[b] *School of Physics and Engineering, Henan University of Science and Technology, Luoyang 471023, P. R. China. E-mail: guoling.li@gmail.com*

[c] *College of Engineering and Applied Sciences, Nanjing University, Nanjing 210093, P. R. China*

[d] *Faculty of Informatics and Engineering, The University of Electro-Communications, Tokyo 182-8585, Japan*

[e] *Key Laboratory for Nano Technology, Nanjing University, Nanjing 210093, P. R. China*

[f] *Faculty of Science, King Abdulaziz University, Jeddah 21589, Saudi Arabia*

[g] *Department of Mathematics, Quaid-I-Azam University, Islamabad 45320, Pakistan*

[h] *Kunshan Sunlaite New Energy Co., Ltd, Kunshan Innovation Institute of Nanjing University, Kunshan, Jiangsu 215347, P. R. China*

*Corresponding author: zhouyong1999@nju.edu.cn (Y. Zhou); guoling.li@gmail.com (G.-L. Li)

Computational details:

Density functional theory (DFT) calculations are done using the projector-augmented wave method and a plane-wave basis set as implemented in the Vienna Ab initio Simulation Package (VASP).[1,2] The valence configurations are treated as $1s^1$ for H, $2s^22p^4$ for O, $3d^84s^1$ for Co, $3d^94s^1$ for Ni, and $4d^75s^1$ for Ru. The Bayesian Error Estimation Functional with van der Waals correlation (BEEF–vdW) is employed.[3] The cutoff energy for plane-wave basis functions is 550 eV. By substituting half Co atoms with Ni atoms within the inverse spinel structure of $NiCo_2O_4$ (JCPDS No. 20-0781), the bulk structure of Ni_2CoO_4 is generated via the Special Quasirandom Structures (SQS) method, which has been widely used to determine the atomic distributions in solid solutions.[4] The bulk lattice parameters of NiO and RuO_2 are fully optimized based on experimental data (NiO JCPDS No. 47-1049, RuO_2 JCPDS No. 40-1290). Based on the optimized structural parameters, we construct periodic surface slabs with six to eight Co/Ni or Ru layers separated by at least 16 Å of vacuum for Ni_2CoO_4 (001), NiO (100) and RuO_2 (110). Atomic positions within the top three layers of the slabs are allowed to relax in OH*, O* and OOH* binding energy calculations. All calculations are done in Γ-centered Monkhorst–Pack *k*-point meshes with a reciprocal-space resolution of 0.15 $Å^{-1}$. The energy convergence is 10^{-5} eV and the force convergence 0.01 eV/Å.

As is known, catalytic activity of the material is determined by the binding energies of the reaction intermediates to the active sites of the catalyst. In the oxygen evolution reaction, OH*, O* and OOH* intermediates are involved. To estimate the adsorption free energies ΔG of different intermediate at zero potential and pH = 0, we calculate the binding energies ΔE of each individual intermediate and corrected them with zero point energy (ZPE) and entropy (TS) using $\Delta G = \Delta E + \Delta ZPE - T\Delta S$.[5] Here, we use the computational hydrogen electrode (CHE) model, which exploits that the chemical potential of a proton-electron pair is equal to gas-phase H_2 at standard conditions. As the ground state of the O_2 is poorly described in DFT calculations we use gas phase

H_2O and H_2 as reference states as they are readily treated in the DFT calculations. The entropy for H_2O is calculated at 0.035 bar which is the equilibrium pressure of H_2O at 300 K. The free energy of this state is therefore equal to that of liquid water. [5]

The theoretical overpotential η is defined as the difference between the limiting potential and equilibrium potential. In the oxygen evolution reaction, the limiting potential is related to the highest free energy step $\Delta G^{OER} = \mathrm{Max}[(\Delta G_{O*} - \Delta G_{OH*}), (\Delta G_{OOH*} - \Delta G_{O*})]$, and the equilibrium potential is 1.23 V. Thus, we get $\eta = (\Delta G^{OER}/e) - 1.23$ V. [6]

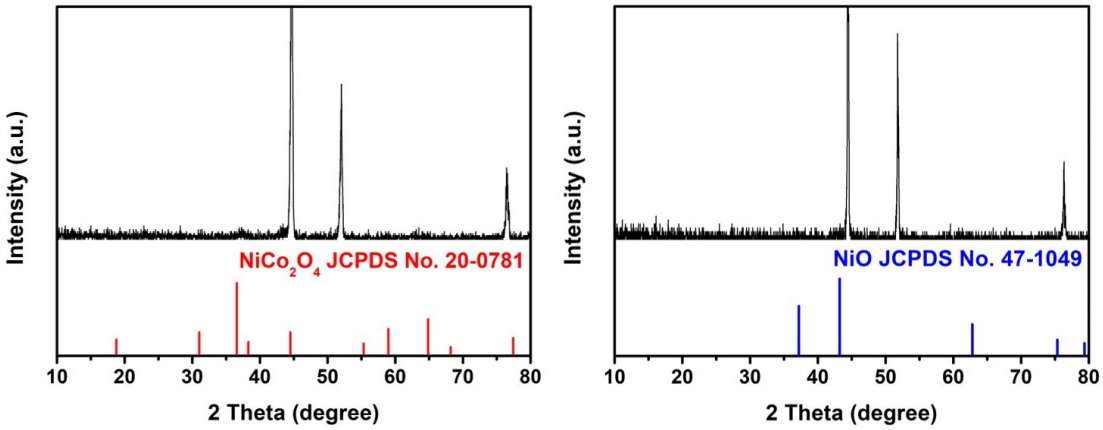

Fig. S1 XRD patterns of (a) $Ni_xCo_{3-x}O_4$/NF and (b) NiO/NF (peaks at 44°, 52° and 76° ascribed to Ni substrate).

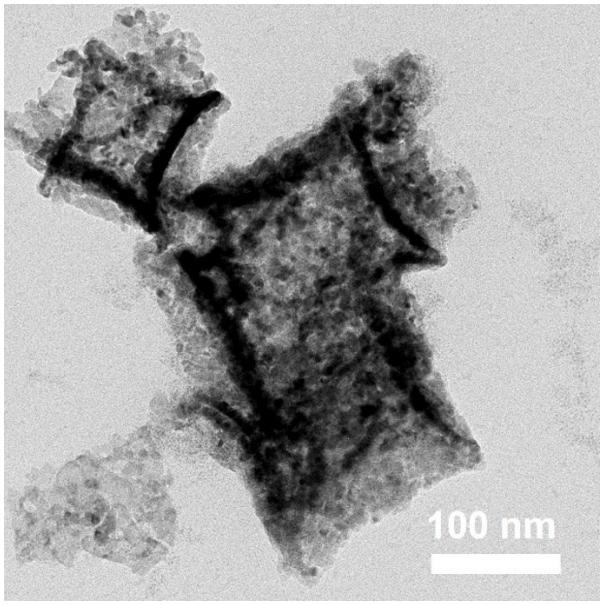

Fig. S2 TEM image of $Ni_xCo_{3-x}O_4$/NF.

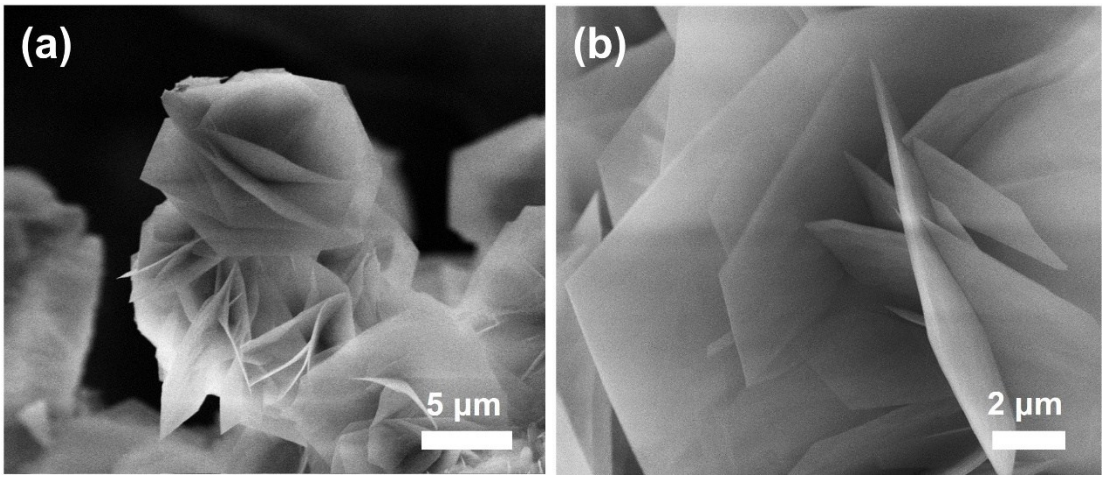

Fig. S3 (a) and (b) FESEM images of NiO/NF.

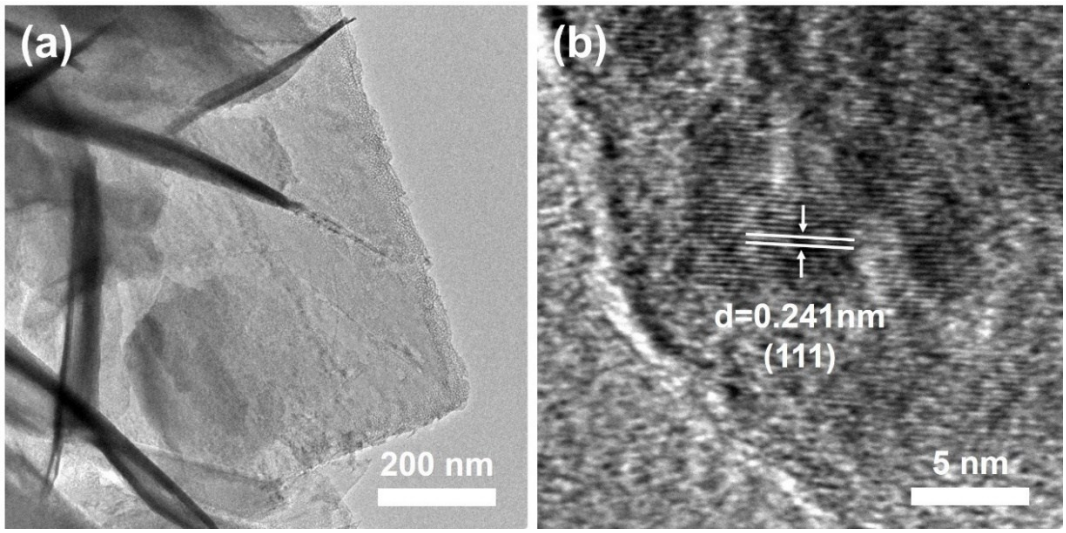

Fig. S4 (a) TEM and (b) HRTEM images of NiO/NF.

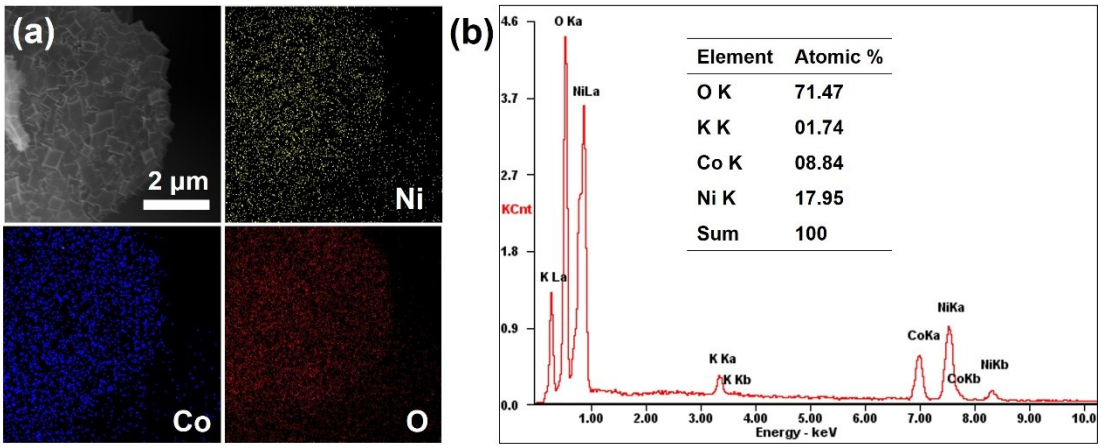

Fig. S5 SEM-EDX (a) elemental mapping and (b) spectrum of $Ni_xCo_{3-x}O_4$. (Trace amount of K element was from the residual potassium cations embedded at the interstitial sites of the frameworks.)

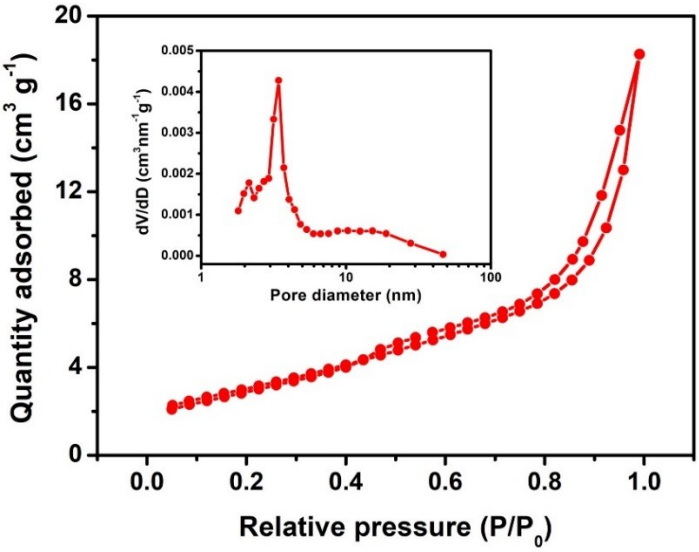

Fig. S6 Nitrogen adsorption-desorption isotherms of $Ni_xCo_{3-x}O_4$/NF (inset corresponding to pore size distribution).

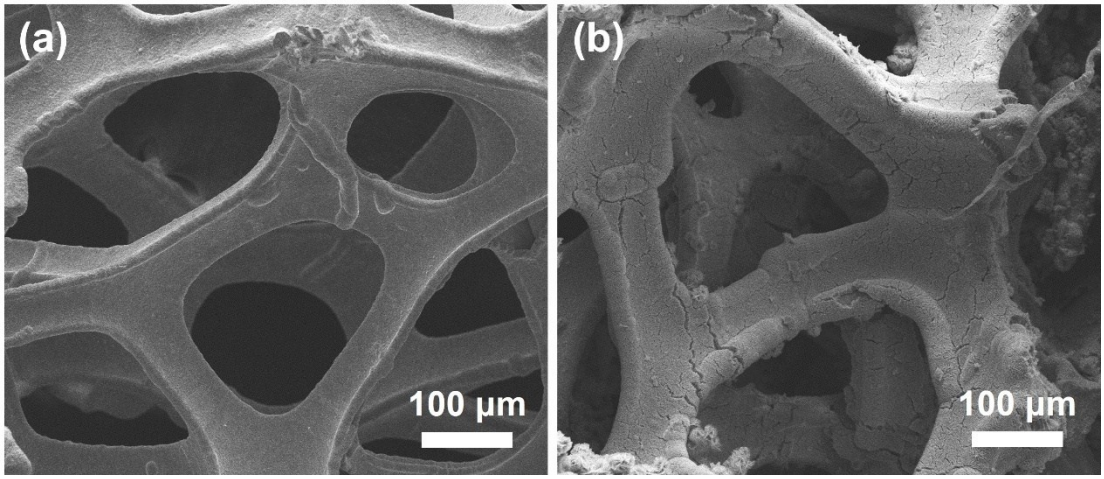

Fig. S7 Low-magnified FESEM images of (a) bare NF and (b) $Ni_xCo_{3-x}O_4$/NF.

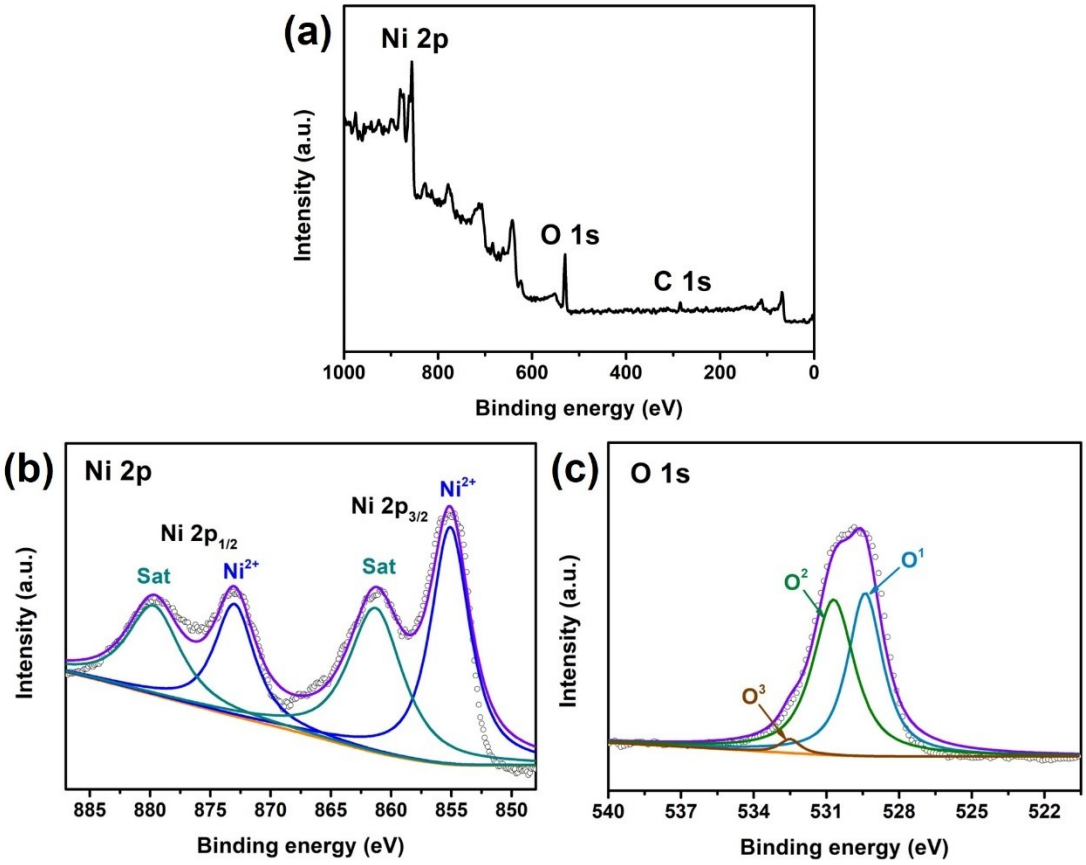

Fig. S8 (a) Full XPS spectrum of NiO and high-resolution spectra of (b) Ni 2p and (c) O 1s.

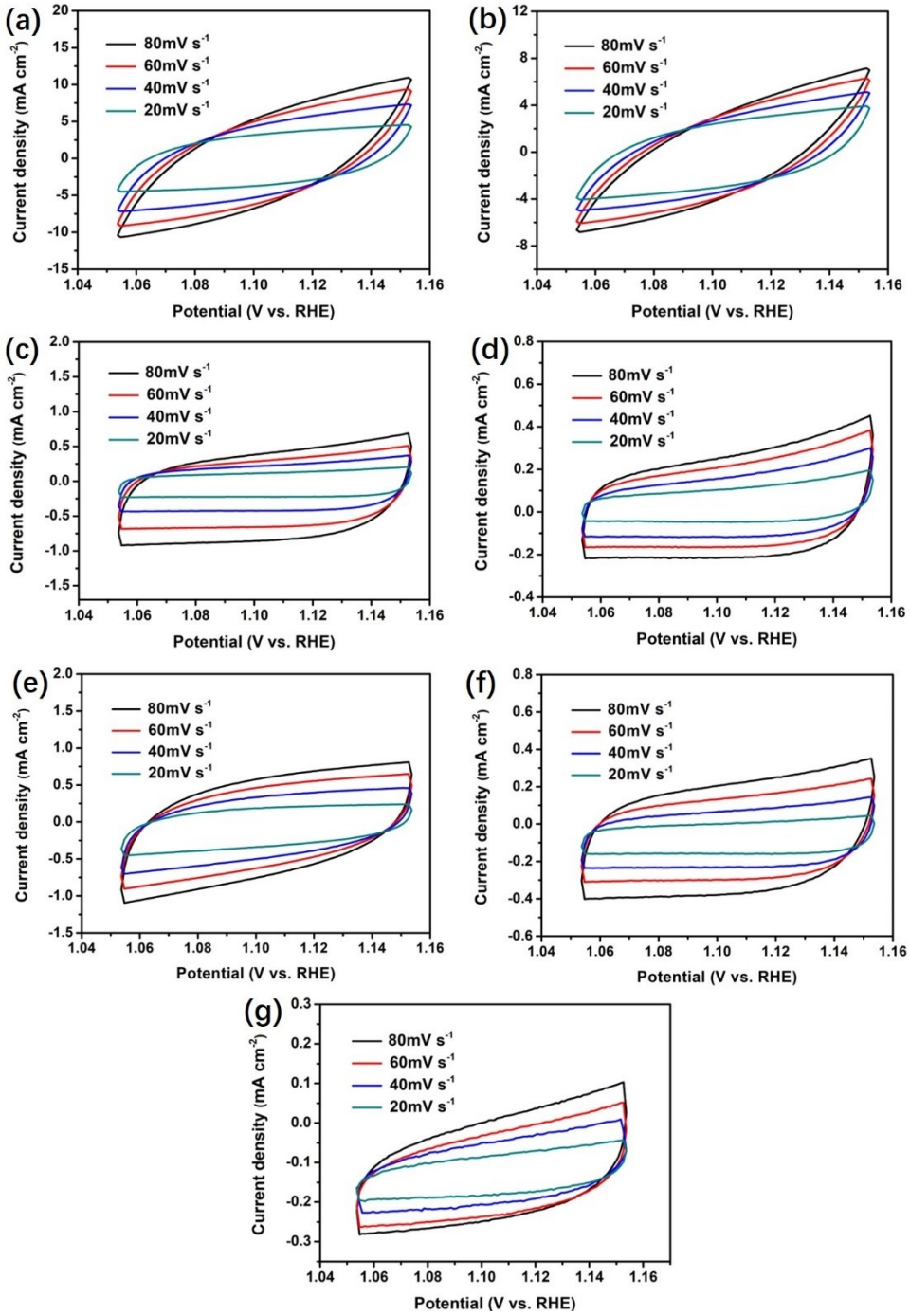

Fig. S9 CV curves of the (a) $Ni_xCo_{3-x}O_4$ /NF, (b) NiO/NF, (c) Ni-Co PBA/NF, (d) $Ni(OH)_2$/NF, (e) RuO_2, (f) NF and (g) $Ni_xCo_{3-x}O_4$ P measured in 1.0 M KOH solution at scan rates from 20 to 80 mV s^{-1}.

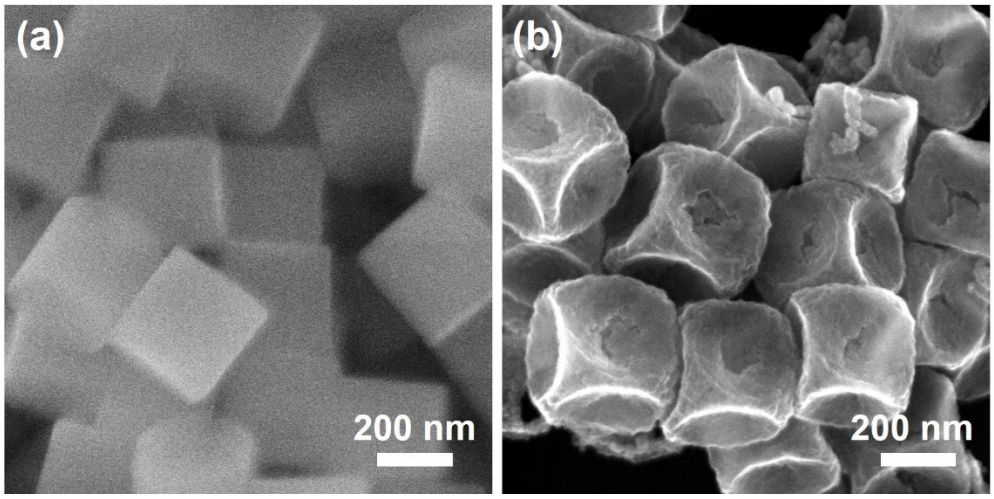

Fig. S10 FESEM images of (a) Ni-Co PBA P and (b) $Ni_xCo_{3-x}O_4$ P.

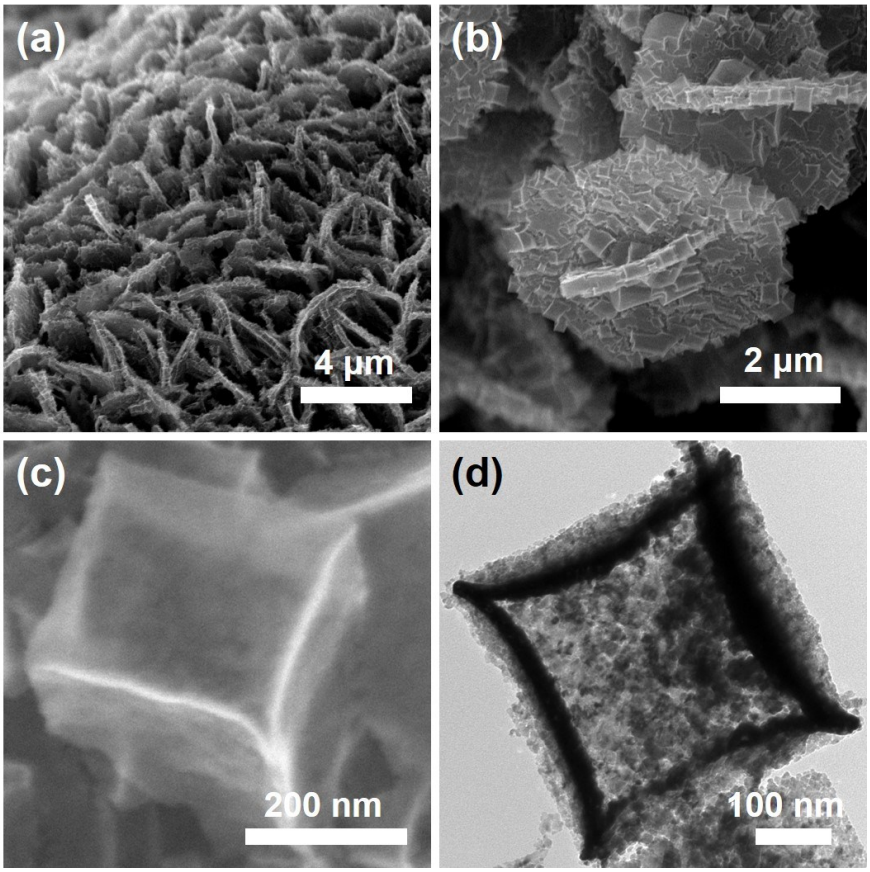

Fig. S11 (a-c) FESEM images and (d) TEM image of $Ni_xCo_{3-x}O_4$/NF after 24 h electrocatalysis.

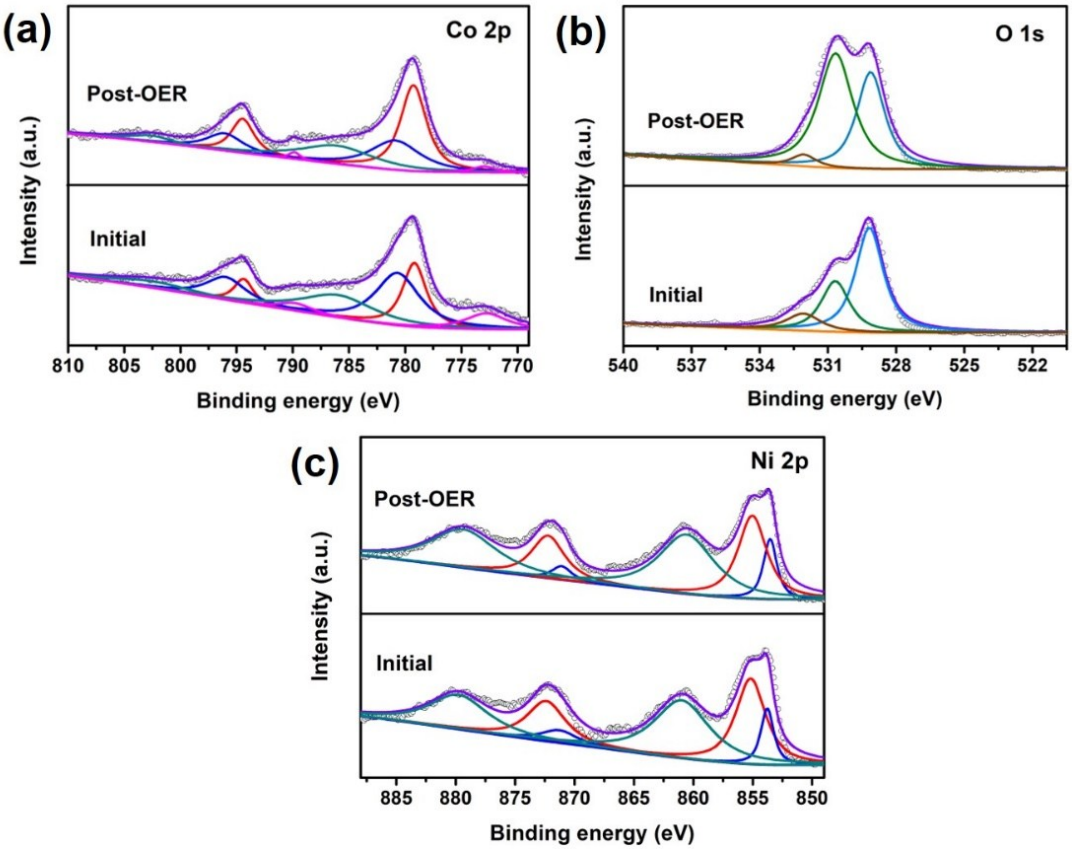

Fig. S12 High-resolution spectra of (a) Co 2p, (b) O 1s and (c) Ni 2p for $Ni_xCo_{3-x}O_4$/NF before and after 24 h electrocatalysis.

Table S1. OER activity[a] of some reported electrocatalysts based on PBAs.

Catalyst	Precursor	Structure	η[b] at 10 mA cm^{-2} (mV)	Tafel Slope (mV dec^{-1})	Ref.
$Ni_xCo_{3-x}O_4$ /NF	Ni-Co PBA arrays on nickel foam (NF)	Hierarchical nanoplate arrays composed of porous and hollow nanocubes on NF	287	88	This work
Ni-Co-Fe PBA	--	Hierarchical hollow nanocuboids	320	49	[7]
$NiO/NiCo_2O_4$	Ni-Co PBA nanocubes	Nanocages consisting of pyramidal walls	380	50	[8]
$CoS_{4.6}O_{0.6}$	Co-Fe PBA nanocubes	Amorphous porous nanocubes	290	67	[9]
Ni_5P_4/Ni_2P	Ni-Ni PBA nanoplates	Porous carbon coated nanoplates	300	64	[10]
Co_3O_4/Co-Fe oxide	ZIF-67/Co-Fe PBA yolk–shell nanocubes	Double-shelled nanoboxes	297	61	[11]
$Co_3S_4@MoS_2$	Co-Fe PBA nanocubes	Hollow core-shell cubic heterostructure	280	43	[12]
NiFeSe@NiSe| O/CC	Ni-Fe PBA@ $Ni_2CO_3(OH)_2$ nanosheet arrays on carbon cloth (CC)	Porous and interconnected heterostructures elaborated with defects on CC	270	63.2	[13]

(a) The electrolyte is 1.0 M KOH expect for **Ref. [7]** (0.1 M KOH).

(b) η is overpotential.

Table S2. Free energies of adsorption for OH*, O* and OOH*, ΔG^{OER} and η for oxygen evolution reaction over $Ni_xCo_{3-x}O_4$ (001), RuO_2 (110) and NiO (100).

Electrocatalyst	ΔG_{OH} (eV)	ΔG_O (eV)	ΔG_{OOH} (eV)	ΔG^{OER} (eV)	η (V)
$Ni_xCo_{3-x}O_4$ (001)	1.05	2.84	3.87	1.79	0.56
RuO_2 (110)	0.49	1.45	3.33	1.88	0.65
NiO (100)	0.22	1.52	3.42	1.90	0.67

References

1 P. E. Blöchl, *Phys. Rev. B*, 1994, **50**, 17953–17979.

2 G. Kresse, J. Furthmüller, *Phys. Rev. B*, 1996, **54**, 11169–11186.

3 J. Wellendorff, K. T. Lundgaard, A. Møgelhøj, V. Petzold, D. D. Landis, J. K. Nørskov, T. Bligaard, K. W. Jacobsen, *Phys. Rev. B*, 2012, **85**, 235149.

4 S. -H. Wei, L. G. Ferreira, J. E. Bernard, A. Zunger, *Phys. Rev. B*, 1990, **42**, 9622–9649.

5 J. K. Norskov, J. Rossmeisl, A. Logadottir, L. Lindqvist, J. R. Kitchin, T. Bligaard, H. Jonsson, *J. Phys. Chem. B*, 2004, **108**, 17886-17892.

6 M. García-Mota, A. Vojvodic, H. Metiu, I. C. Man, H. Y. Su, J. Rossmeisl, J. K. Nørskov, *ChemCatChem*, 2011, **3**, 1607-1611.

7 W. Ahn, M. G. Park, D. U. Lee, M. H. Seo, G. Jiang, Z. P. Cano, F. M. Hassan, Z. Chen, *Adv. Funct. Mater.*, 2018, **28**, 1802129.

8 L. Han, X. -Y. Yu, X. W. Lou, *Adv. Mater.*, 2016, **28**, 4601-4605.

9 P. Cai, J. Huang, J. Chen, Z. Wen, *Angew.Chem.*, 2017, **129**, 4936-4939.

10 X.-Y. Yu, Y. Feng, B. Guan, X. W. Lou, U. Paik, *Energy Environ. Sci.*, 2016, **9**, 1246-1250.

11 X. Wang, L. Yu, B. Y. Guan, S. Song, X. W. Lou, *Adv. Mater.*, 2018, **30**, 1801211.

12 Y. Guo, J. Tang, Z. Wang, Y.-M. Kang, Y. Bando, Y. Yamauchi, *Nano Energy*, 2018, **47**, 494-502.

13 G. Yilmaz, C. F. Tan, Y.-F. Lim, G. W. Ho, *Adv. Energy Mater.*, 2018, 1802983.